Title

mTOR regulates peripheral nerve response to tensile strain

Journal

Journal of Neurophysiology, 117(5)

ISSN

0022-3077

Authors

Love, James M
Bober, Brian G
Orozco, Elisabeth
et al.

Publication Date

2017-05-01

DOI

10.1152/jn.00257.2016

Peer reviewed

J Neurophysiol 117: 2075–2084, 2017.
First published March 1, 2017; doi:10.1152/jn.00257.2016.

RESEARCH ARTICLE | *Glial Cells and Neuronal Signaling*

mTOR regulates peripheral nerve response to tensile strain

James M. Love,[1] Brian G. Bober,[2] Elisabeth Orozco,[3,4] Amanda T. White,[3] Shannon N. Bremner,[3,4] Richard M. Lovering,[5] Simon Schenk,[3] and Sameer B. Shah[2,3,4]

[1]*Fischell Department of Bioengineering, University of Maryland, College Park, Maryland;* [2]*Department of Bioengineering, University of California-San Diego, La Jolla, California;* [3]*Department of Orthopaedic Surgery, University of California-San Diego, La Jolla, California;* [4]*Veterans Affairs San Diego Healthcare System, San Diego, California; and* [5]*Department of Orthopaedics, University of Maryland School of Medicine, Baltimore, Maryland*

Submitted 28 March 2016; accepted in final form 25 February 2017

Love JM, Bober BG, Orozco E, White AT, Bremner SN, Lovering RM, Schenk S, Shah SB. mTOR regulates peripheral nerve response to tensile strain. *J Neurophysiol* 117: 2075–2084, 2017. First published March 1, 2017; doi:10.1152/jn.00257.2016.—While excessive tensile strain can be detrimental to nerve function, strain can be a positive regulator of neuronal outgrowth. We used an in vivo rat model of sciatic nerve strain to investigate signaling mechanisms underlying peripheral nerve response to deformation. Nerves were deformed by 11% and did not demonstrate deficits in compound action potential latency or amplitude during or after 6 h of strain. As revealed by Western blotting, application of strain resulted in significant upregulation of mammalian target of rapamycin (mTOR) and S6 signaling in nerves, increased myelin basic protein (MBP) and β-actin levels, and increased phosphorylation of neurofilament subunit H (NF-H) compared with unstrained (sham) contralateral nerves ($P < 0.05$ for all comparisons, paired two-tailed *t*-test). Strain did not alter neuron-specific β3-tubulin or overall nerve tubulin levels compared with unstrained controls. Systemic rapamycin treatment, thought to selectively target mTOR complex 1 (mTORC1), suppressed mTOR/S6 signaling, reduced levels of MBP and overall tubulin, and decreased NF-H phosphorylation in nerves strained for 6 h, revealing a role for mTOR in increasing MBP expression and NF-H phosphorylation, and maintaining tubulin levels. Consistent with stretch-induced increases in MBP, immunolabeling revealed increased S6 signaling in Schwann cells of stretched nerves compared with unstretched nerves. In addition, application of strain to cultured adult dorsal root ganglion neurons showed an increase in axonal protein synthesis based on a puromycin incorporation assay, suggesting that neuronal translational pathways also respond to strain. This work has important implications for understanding mechanisms underlying nerve response to strain during development and regeneration.

NEW & NOTEWORTHY Peripheral nerves experience tensile strain (stretch) during development and movement. Excessive strain impairs neuronal function, but moderate strains are accommodated by nerves and can promote neuronal growth; mechanisms underlying these phenomena are not well understood. We demonstrated that levels of several structural proteins increase following physiological levels of nerve strain and that expression of a subset of these proteins is regulated by mTOR. Our work has important implications for understanding nerve development and strain-based regenerative strategies.

Address for reprint requests and other correspondence: S. B. Shah, 9500 Gilman Dr., MC 0863, La Jolla, CA 92093 (e-mail: sbshah@ucsd.edu).

peripheral nerve; strain; mTOR; cytoskeleton; myelin; neurofilament; rapamycin

EXCESSIVE TENSILE STRAIN (stretch) or high strain rates can damage peripheral nerves and their component neurons, often irreversibly (Kwan et al. 1992; Wall et al. 1992); however, neurons also possess a remarkable ability to accommodate and respond to moderate levels of tensile loading. Nerves are stretched during rapid phases of organism growth (Weiss 1941), bear acute strains up to 25% during joint movement (Boyd et al. 2005), and also adapt to more persistent strain, such as that occurring during limb lengthening (Ikeda et al. 2000). Consistent with the latter, in vitro evidence suggests that strained axons can increase both their growth capacity and rate of elongation (Bray 1984; Lamoureux et al. 1998; Pfister et al. 2004).

These concepts have recently been translated into strain-based neuroregenerative strategies, with varied success (Chuang et al. 2013; Hentz et al. 1993; Iwata et al. 2006). Axons gain volume rather than simply thinning while under strain (Loverde et al. 2011) and thus require an increase of cellular material to support this expansion. Such a response is analogous to that occurring during axonal outgrowth during development or following injury, in which the production of many proteins, including those associated with the cytoskeleton, is increased (Donnelly et al. 2013; Eng et al. 1999; Tetzlaff et al. 1988). In addition, internodes also lengthen in response to strain (Abe et al. 2004; Abe et al. 2002) suggesting that myelinating Schwann cells also respond to deformation. Despite these compelling observations, our ability to optimize strain-driven regenerative strategies is limited by a poor understanding of biological mechanisms underlying the response of nerves to strain.

Local protein synthesis provides an efficient way to mobilize structural elements required for increased neuronal volume. To this end, a number of mRNAs encoding cytoskeletal proteins are present locally within the axonal compartment, including β-actin, tubulin, and neurofilament heavy subunit (NF-H) (Eng et al. 1999; Olink-Coux and Hollenbeck 1996; Sotelo-Silveira et al. 2000). These transcripts appear to be translated under conditions of stress. For example, severed axons require axonal protein synthesis to regenerate (Park et al. 2010; Verma et al.

2005; Zheng et al. 2001), in a mammalian target of rapamycin (mTOR)-dependent manner. Consistent with these findings, suppression of phosphatase and tensin homolog (PTEN), an inhibitor of mTOR, enhances axonal elongation (Ning et al. 2010). A role for mTOR in regulating strain-associated axonal expansion has not yet been tested. However, several other tissue systems, including striated muscle, respond to strain by activating mTOR-dependent protein synthetic pathways, which are initiated by focal adhesion kinase (FAK) phosphorylation (Klossner et al. 2009).

Considering the importance of mTOR in axonal extension as well as its role in responding to strain in nonneuronal cells, we hypothesized that applied peripheral nerve strain activates mTOR-mediated signaling pathways, resulting in increased synthesis of structural proteins within the nerve. Our data support this hypothesis in both axons and myelinating Schwann cells.

MATERIALS AND METHODS

Animal Care

Animals were used under protocols approved by the University of California-San Diego (UCSD) Institutional Animal Care and Use Committee. For in vivo experiments, adult male Sprague-Dawley rats between the ages of 10 and 13 wk were utilized. For in vitro experiments, dorsal root ganglia (DRGs) from embryonic day 18 (E18) Sprague-Dawley rats were cultured. All adult animals were euthanized by asphyxiation with CO_2 followed by confirmation via removal of major organs. Embryonic rats were euthanized by decapitation.

Animal Surgery and Nerve Strain

Anesthesia was induced with 5% isoflurane and maintained for the duration of the experiments at 1.5–3% isoflurane. Thermoregulation was achieved using an aquathermal pad, and heart rate and respiratory rate were monitored throughout the surgery. The experimental limb in which the nerve was strained was randomly assigned, and the contralateral limb was used for paired comparison. The control nerve was always exposed first, no more than 5–7 min before the strained nerve. The rationale for this sequence was that the sham experienced minimally more stress due to slightly increased duration of exposure, and thus our comparisons were, if anything, conservative. Surgery consisted of sciatic nerve exposure through separation of the fascial band of the biceps femoris. The nerve was then freed from the tissue bed by removing superficial fascia. A custom wedge was placed beneath the sciatic nerve, creating strain by elevating the nerve from the tissue bed (Fig. 1, *A* and *B*). By using this method, potential damage associated with grasping or clamping strategies for nerve lengthening was avoided. In addition, regional redistributions of strain or torsion incurred by manipulating joint positions were avoided. Changes in the spacing between surface markings on the epineurium, created with a tissue marker, were used to measure strain following nerve elevation relative to before nerve elevation. Strain was measured along the longitudinal axis of the nerve. Nerves were strained for a period of either 15 min (acute signaling) or 6 h (altered protein expression) depending on the desired outcome measurement. Limb positioning was maintained in a neutral position throughout the period of strain, with knee at ~40° flexion and ankle at 10° of plantarflexion. During stretch, nerves were continually soaked in a PBS-soaked piece of gauze to ensure that the nerve did not dehydrate during experimentation. The strained section of the sciatic nerve was excised, flash frozen in liquid nitrogen-cooled isopentane, and stored at −80°C for future processing. Sham surgeries were performed on contralateral limbs, exposing and freeing the sciatic nerve without wedge insertion.

Rapamycin Treatment

To inhibit mTOR activity, rats were injected intraperitoneally with 5 mg/kg rapamycin (J62473; Alfa Aesar) in a solution consisting of 1 mg/ml rapamycin, 5% vol/vol ethanol, 4% vol/vol Tween 80, 4% vol/vol polyethylene glycol in sterile water (as described in Eshleman et al. 2002). Carrier control rats were injected with the same solution without rapamycin.

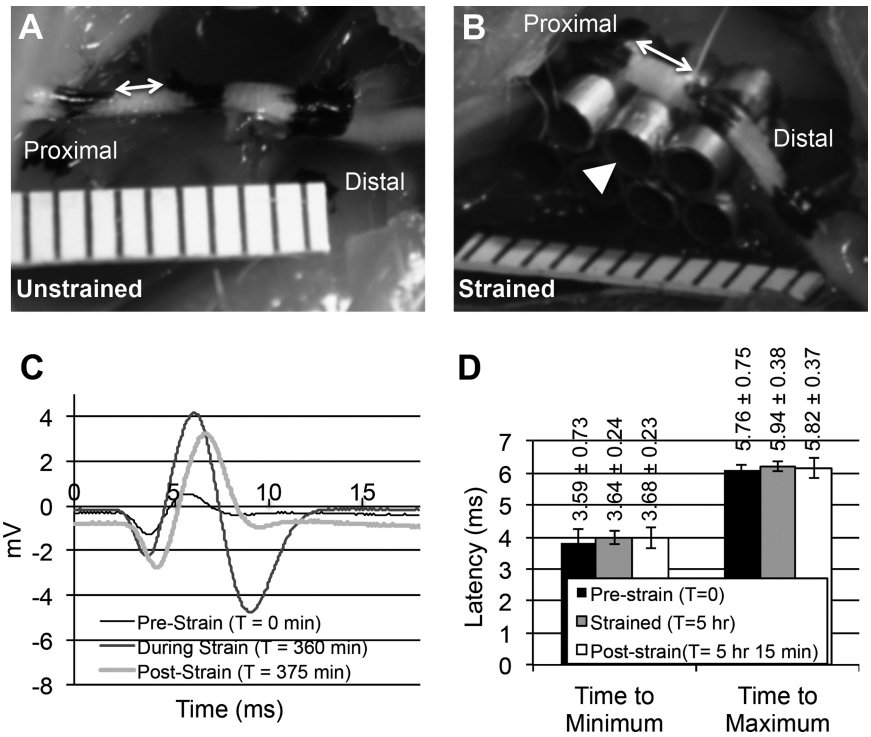

Fig. 1. Experimental setup and electrophysiology. *A*: sciatic nerves were marked and imaged following exposure for baseline reference. *B*: insertion of custom wedge strained the nerve locally without causing damage. Markings were used to ensure consistent strain of the nerves. Double-headed arrows in *A* and *B* represent distances between the edges of ink markings, used to calculate strain. Note that images provided are from different angles and were included to show device (arrowhead) insertion. Actual measurements were made from an image captured from above the nerve, with ruler in same plane as nerve. *C*: sample EMG recordings from the tibialis anterior (TA) displays characteristic depolarization and hyperpolarization following sciatic nerve stimulation. Sample traces from before, during, and after stretch are shown. Increased amplitude during and after stretch likely reflects changes in contact geometry of electrode with the nerve. *D*: latency measurements, made from time of stimulation to time of minima and maxima of the recording trace, revealed no significant differences between pre- and poststretch (paired *t*-test, means ± SE, $n = 3$, all $P > 0.05$).

Tissue Homogenization and Sample Preparation

Individual nerves were homogenized in 150 μl of homogenization buffer consisting of 20 mM Tris·HCl, 150 mM NaCl, 1% vol/vol nonyl phenoxypolyethoxylethanol (NP-40), 20 mM NaF, 2 mM EDTA, 2.5 mM sodium polyphosphate (NaPP), 20 mM β-glycerophosphate, and 10% glycerol (Schenk et al. 2011; White et al. 2013). Homogenization buffer was supplemented with cOmplete (04693116001; Roche) and phosSTOP (04906845001; Roche) to inhibit protein degradation and dephosphorylation. Whole protein levels were quantified by BCA protein assay (Pierce), then samples were diluted with homogenization buffer to 1 μg/μl total protein, supplemented with Laemmli sample buffer at 3:1 (sample to buffer). Samples were boiled for 10 min before storage at −80°C.

Western Blotting

Samples were removed from −80°C and heated at 60°C for 6 min. Proteins were separated within 3–8% Tris-acetate gels (Bio-Rad Laboratories, 20 μg total protein per well, based on results from BCA protein assay), for 95 min at 110 V. Following electrophoresis, proteins were transferred to nitrocellulose membranes (2 h at 4°C and 200 mA). Ponceau S (59803; Cell Signaling Technology) was used to confirm that no gross errors in pipetting or transfer occurred. Membranes were blocked with 5% nonfat milk, washed, then incubated primary antibody overnight at 4°C. The membrane was again washed, then incubated for 1 h in secondary antibody (1:1,000). Proteins were visualized using ECL (Pierce). Image capture and quantification of Western blots were performed using ImageLab software on a Chemidoc imager (Bio-Rad). Phosphorylated levels of a given protein were normalized to the total levels of the protein. For this analysis, phosphorylated proteins were probed, membranes were stripped, and total protein levels for the corresponding protein were probed on the same membrane. In addition, we normalized total protein levels to those of GAPDH (Ning et al. 2010). Primary antibodies used were: pmTOR^{Ser2448} (5536P; Cell Signaling), total mTOR (2983P; Cell Signaling), pFAK^{Y397} (44624G; Life Technologies), total FAK (05537; Millipore), pS6$^{Ser240/244}$ (2215S; Cell Signaling), total S6 (2317S; Cell Signaling), β-actin (A5060; Sigma-Aldrich), tubulin (T9026; Sigma-Aldrich), SMI-31 (ab24573; abcam), GAPDH, NF-H, Tuj1 (NC0475670; Covance), myelin basic protein (MBP; MAB386; Millipore). Horseradish peroxidase-conjugated secondary antibodies (Zymed) appropriate for each primary antibody were used.

Electrophysiology

Methods were similar to those of Restaino et al. 2014, excepting the use of the tibialis anterior (TA) to record muscle response to nerve stimulation. Briefly, following sciatic nerve exposure, a miniature bipolar hook electrode (501650; Harvard Apparatus) was positioned proximal to the strained region. The TA was exposed and needle recording electrodes (Grass F-E2) were positioned adjacent to the endplate zone (Westerga and Gramsbergen 1993). A ground needle electrode was placed in the contralateral limb. A Grass SD9 stimulator (Grass Astromed Technologies) was used to generate stimulation pulses. Parameters were chosen to minimize the applied voltage, while maintaining a recordable and consistent EMG response; these parameters were six monophasic 50-μs duration square pulses at 5 Hz, at an input voltage of 7 V (<10 mA). At each time point, five consecutive recordings were made to ensure consistency of stimulation and recording and averaged together to determine the latency between stimulus and recording. Latency was determined based on the delay between the timed and synchronized stimulation and recordings such as those shown in Fig. 1. Unstrained measurements were made with the nerve in a neutral configuration, with knee at ~40° flexion and ankle at 10° of plantarflexion. Wedges were used to impose strain during the 360-min period as above. Measurements were made at the following time points in the following order: unstrained at $t = 0$ min, strained at $t = 0$ min, strained at $t = 15$ min, unstrained at $t = 15$ min, strained at $t = 360$ min, unstrained at $t = 360$ min, unstrained at $t = 375$ min (i.e., an additional 15-min rest period following wedge removal).

Cell Culture

Isolated DRGs were digested in trypsin for 30 min. Five milliliters of fresh culture medium (MEM + 10% FBS + 1% penicillin/streptomycin/neomycin + 2% B27 + 50 ng/ml NGF) were added to the DRGs to halt trypsin activity. Cells were spun down at 90 *g*. Medium was aspirated and cells were resuspended in fresh medium. DRGs were plated on custom microfluidic polydimethylsiloxane (PDMS) wells (Bober et al. 2015). Wells were functionalized by (3-aminopropyl) triethoxysilane treatment followed by laminin coating in the presence of 1-ethyl-3-(3-dimethylaminopropyl) carbodiimide.

In Vitro Protein Synthesis Assay

One day postplating, neuronal protein synthesis was examined by puromycin treatment, in a manner analogous to that previously deployed for nonneuronal cells (Schmidt et al. 2009). Medium was removed and replaced with medium containing 10 μg/ml puromycin. Cells were incubated in puromycin medium at 37°C for 10 min, a time point at which neurons remained viable. After incubation, cells were washed 3× with fresh medium and then allowed to recover for 50 min. At this point cells were either left unstrained or strained ~20% by application of vacuum pressure to the microfluidic chamber. Cells were stretched using published methods (Bober et al. 2015). Briefly, stretch was imposed at a rate of ~0.5%/s, to prevent possible damage from rapid extension, and the membrane was maintained in a stretched position throughout the experiment. For rapamycin experiments, medium was supplemented with 10 μM rapamycin during the incubation and recovery period. Cells were fixed within 5 min of release and immunostained to determine localization and degree of puromycin incorporation into newly synthesized proteins. For each cell analyzed, mean pixel intensity was calculated along the axon. A region of interest was drawn manually around the axon, excluding the cell body from the axonal hillock, but including the growth cone. Following background subtraction, the resultant region of interest was thresholded using Otsu's method (ImageJ, National Institutes of Health), and the mean intensity of positive pixels was calculated.

Immunocytochemistry

Cells were fixed with 4% vol/vol paraformalin in PBS for 10 min at 37°C, washed, and then permeabilized with 0.2% vol/vol Triton X-100 in PBS for 5 min. Cultures were washed 3× in PBS. Cells were blocked in 10% vol/vol FBS and 1% BSA wt/vol in PBS for 30 min. Blocking buffer was removed and cells were incubated at room temperature in primary antibody in blocking buffer for 1 h followed by 3× wash in PBS and 1 h incubation in secondary antibody diluted in blocking buffer followed by 3× wash in PBS.

Tissue Processing and Immunohistochemistry

Nerves were pinned to cork and flash frozen in liquid nitrogen cooled 2-methylbutane following a 6-h period of strain. Nerves were stored at −80°C until sectioned. Nerves were embedded in OCT compound (Tissue-Tek) and 10 μm cross sections were prepared and placed onto Superfrost Plus (ThermoFisher) slides.

Samples on slides were circled using an ImmEdge pen (Vector Laboratories) to form a hydrophobic boundary. Following immersion in deionized water, slides were fixed for 45 min in 10% formalin, then permeabilized in 0.2% Triton X-100. Slides were blocked for 20 min

in blocking buffer, then placed in primary antibody for 1 h at room temperature; 3× washes with PBS were used between each step. Secondary antibody was applied for a period of 1 h. Samples were coverslipped with VectaShield and sealed with nail polish. Phospho-S6 and Mouse MBP primary antibodies (from Western blots) were used at a dilution of 1:1,000 in blocking buffer with Alexa Fluor 488 goat-anti-mouse and Alexa Fluor 594 goat anti-rabbit secondary antibodies, which were diluted 1:200 in blocking buffer.

Confocal Imaging

Images were obtained using a Leica SP5 system equipped with an argon laser for excitation at 488 nm and a HeNe laser for excitation 594 nm. Emission was captured from 500 to 550 nm for 488-nm excitation and between 600 and 650 nm for 594-nm excitation. Laser power and gains were kept constant to allow for adequate image acquisition and quantitative comparisons (Table 1). Images were captured at a resolution of 1,024×1,024 pixels and line averaged 3× for noise reduction.

Statistics

Paired *t*-tests were used to compare contralateral strained and unstrained nerves (Excel; Microsoft). Two-way ANOVAs (analysis of variance) were used to compare the effects of rapamycin treatment and strain on protein levels or signaling, with Tukey's HSD used to compare individual means post hoc. Experimental groups of eight rats were used for all experiments except where otherwise noted; this sample size was selected conservatively, based on a power calculation that required six samples/group ($\alpha = 0.05$, $\beta = 0.2$).

RESULTS

Model for In Vivo Nerve Strain

We developed methodology to strain rat sciatic nerves without incurring damage associated with clamping or grasping the nerve. Insertion of a custom-made isosceles trapezoidal wedge into the underlying nerve bed (Fig. 1*B*) imparted a consistent tensile nerve strain on the top edge of the wedge by creating a four-point bending configuration on the nerve [conceptually analogous to bow-stringing of axons (Dennerll et al. 1989) or nerve elongation with a tissue expander (Arnaoutoglou et al. 2006)]. Rounded corners of the wedge minimized any nerve tethering and allowed a gradual reduction of strain along regions of the nerve descending from the wedge. Based on the spacing between dots painted onto the epineurium, strains of 11.24 ± 0.95% (mean ± SE, $n = 5$) were measured, a magnitude approaching, but not exceeding, upper limits of physiological strains (Boyd et al. 2005).

During this procedure, though decompression may have affected the segmental blood supply to the nerve, we did not observe any indication of substantial vascular impairment, including pooling blood, changes of nerve or muscle coloration, or changes in heart or pulse rate. To confirm that nerves did not experience injurious compression or damage over the course of the experiment, conduction latencies to the TA were measured, following stimulation of the sciatic nerve proximal to the site of strain (Fig. 1*C*). Comparison of prestretch latencies with those after 300 min, a time point equal to the longest time point in all other experiments, showed no significant differences in latencies to primary or secondary peaks (Fig. 1, *C* and *D*). Additionally, while signal amplitude was variable from time point to time point (though not for repeated measurements within a time point), at no point did we see a significant reduction in peak amplitude between prestretch (4.26 ± 2.22 V), 5-h stretch (7.09 ± 1.40 V), and recovered (6.49 ± 1.38 V). The apparent increase in amplitude during stretch is likely a result of increased recruitment of fibers by the electrode due to flattening of the nerve. Collectively, these data indicate that our nerve stretch model does not result in appreciable changes to neurovascular function and that a physiologically reasonable surgical plane was maintained throughout the experiment.

Table 1. *Power/gain settings for immunofluorescence*

	Power	Gain
MBP (488)	30%	939.0
pS6 (594)	70%	709.0
SMI31 (488)	30%	815.8
Puromycin (488)	30%	543.8

Laser power and gain settings were kept constant for all samples to allow for quantification of immunofluorescence.

mTOR Pathway Activation and Cytoskeletal Protein Expression Following Nerve Strain

To determine whether mTOR-associated translational pathways were activated in strained nerves away from neuronal cell bodies, we first used Western blot analysis to examine the response of FAK and mTOR activation levels following 15 min of applied strain. Consistent with other model systems, a strong trend toward rapid mTOR activation with strain was observed by a 40% increase in the p-mTOR/mTOR ratio for strained nerves compared with unstrained ($P = 0.070$, paired *t*-test; Fig. 2, *A* and *B*). However, FAK signaling was unresponsive at this early time point as well as at later time points up to 6 h (data not shown, $n = 4$), suggesting an alternate mode of initiation (Fig. 2, *A* and *B*). Following 6 h of applied strain, mTOR signaling persisted, with an increase of 37% over unstrained nerves ($P = 0.002$, paired *t*-test; Fig. 2, *C* and *D*). Consistent with this activity, we also observed a 28% increase in activation of S6, a translational regulator downstream of mTOR, in strained compared with unstrained nerves at 6 h ($P = 0.014$, paired *t*-test; Fig. 2, *C* and *D*). Total mTOR and S6 levels trended slightly higher after stretch, though they were not significantly different compared with controls (Fig. 2, *F* and *G*); together, these data indicate that stretch results in increased activation of an equal or larger pool of total mTOR/S6 than that present in the absence of stretch.

We then tested whether strain induced a corresponding increase in cytoskeletal protein expression. We focused on expression of β-actin, neurofilament heavy subunit (NFH) and tubulin, each hypothesized to be synthesized locally in neurons (Eng et al. 1999; Olink-Coux and Hollenbeck 1996; Sotelo-Silveira et al. 2000). Cytoskeletal protein levels were normalized to GAPDH, a noncytoskeletal marker. Following 6 h of strain, relative to unstrained contralateral nerves, we observed increases in β-actin (130%; $P = 0.035$, paired *t*-test; Figs. 2, *E* and *F*), but no significant increase in neuron-specific tubulin Tuj1 ($P = 0.086$), total tubulin ($P = 0.466$), or NF-H ($P = 0.755$) following strain application.

Localization of S6 signaling. Because of the various cell types within nerve tissue, it was important to determine the

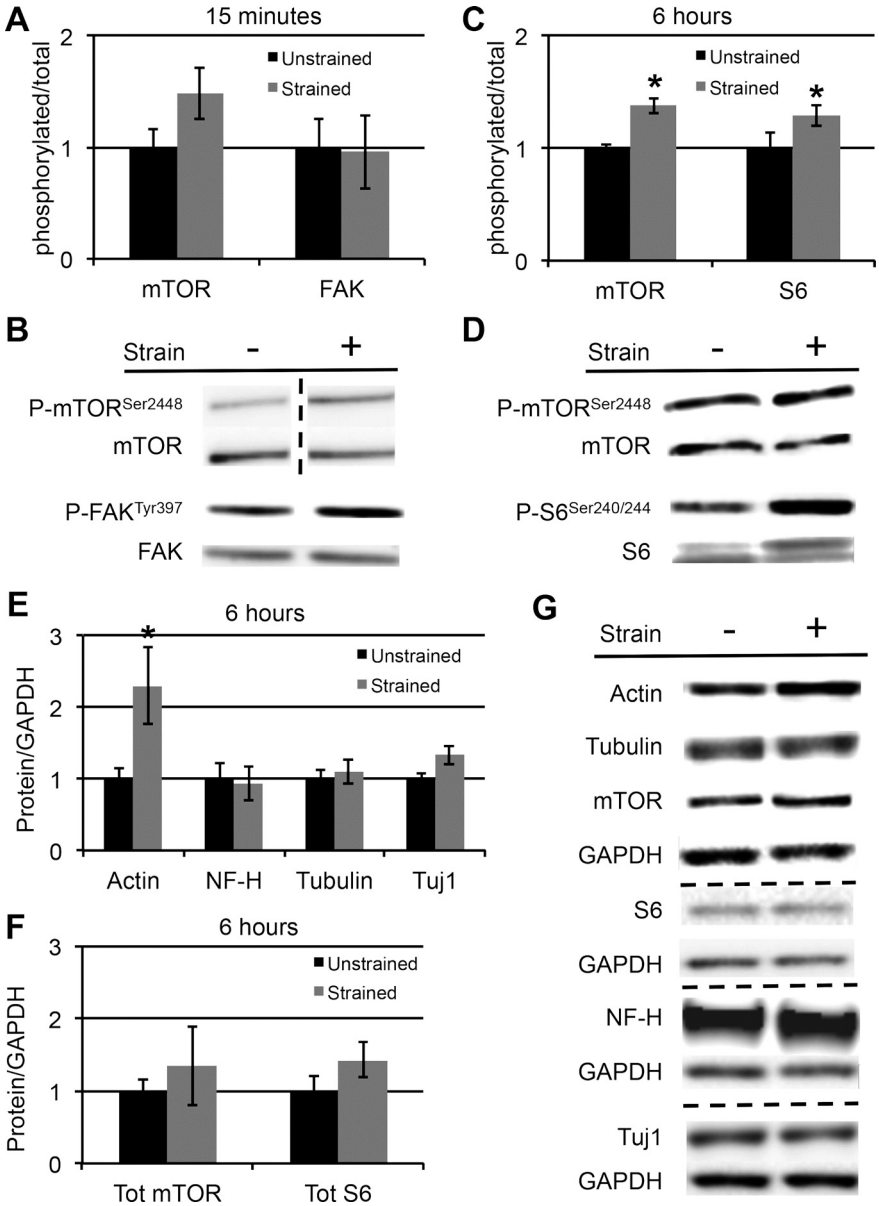

Fig. 2. Strain-induced signaling and protein expression. *A*: application of strain for 15 min revealed a trend toward increased mTOR phosphorylation with constant levels of FAK signaling ($n = 4$) as revealed by Western blotting (*B*). *C*: following 6 h of strain application, a significant increase was observed in both mTOR and S6 phosphorylation levels following the application of strain as revealed by Western blotting (*D*). *E* and *F*: β-actin levels significantly increased following application of strain while tubulin and total mTOR and total S6 levels remained constant as revealed by Western blotting. *G*: sample blots for each protein of interest. $^*P < 0.05$, paired *t*-test; means ± SE; all graphs normalized to unstrained levels.

localization of the increased phospho-S6 signaling. Immunolabeled cross sections of rat sciatic nerves harvested after sham treatment or stretch revealed an increase in S6 signaling in strained nerves (Fig. 3, *C* vs. *D* and *G*). Interestingly, colocalization of this signal with increased MBP signaling suggests that much of the increased S6 signaling occurred in the Schwann cells (Fig. 3, *B* and *D*). Quantification of immunofluorescence showed an increase in MBP levels (Fig. 3, *A*, *B*, and *G*; $P = 0.049$; unpaired *t*-test, $n = 3$) and a trend toward increased phospho-S6 levels ($P = 0.073$) following strain application. As myelination is thought to also influence neurofilament phosphorylation (de Waegh et al. 1992; Hsieh et al. 1994), we also probed for levels of phosphorylated neurofilaments; immunofluorescence also revealed an apparent increase in SMI-31 labeling in strained nerves (Fig. 3, *D* and *H*), though differences in the dimensions of the rat nerves examined precluded accurate analysis. Therefore, to confirm increases in MBP and phosphorylated neurofilaments, we performed Western blots (Fig. 3, *H* and *I*). Significant increases with strain were observed for both MBP ($P = 0.014$) and SMI-31 ($P = 0.008$).

Rapamycin Regulation of Protein Levels in Strained Nerves

Given the concurrent increase in mTOR/S6 activation and levels of several proteins following 6 h of strain, we next tested the hypothesis that inhibition of mTOR complex 1 (the mTOR complex associated with activation of S6) by systemic rapamycin administration would suppress these increases. Rapamycin was administered 1 h before the 6-h period of strain application. To confirm rapamycin activity, we examined the level of mTOR activation following strain application by Western blot. Both the contralateral, unstrained nerve (50% reduction; Fig. 4, *A* and *B*) and strained nerves (30% reduction; Fig. 4, *A* and *B*) revealed a significant reduction in mTOR activation. Two-way ANOVA analysis for strain and rapamycin revealed a significant rapamycin-dependent decrease in mTOR activation ($P = 6.86\times10^{-13}$). Additionally, a strain

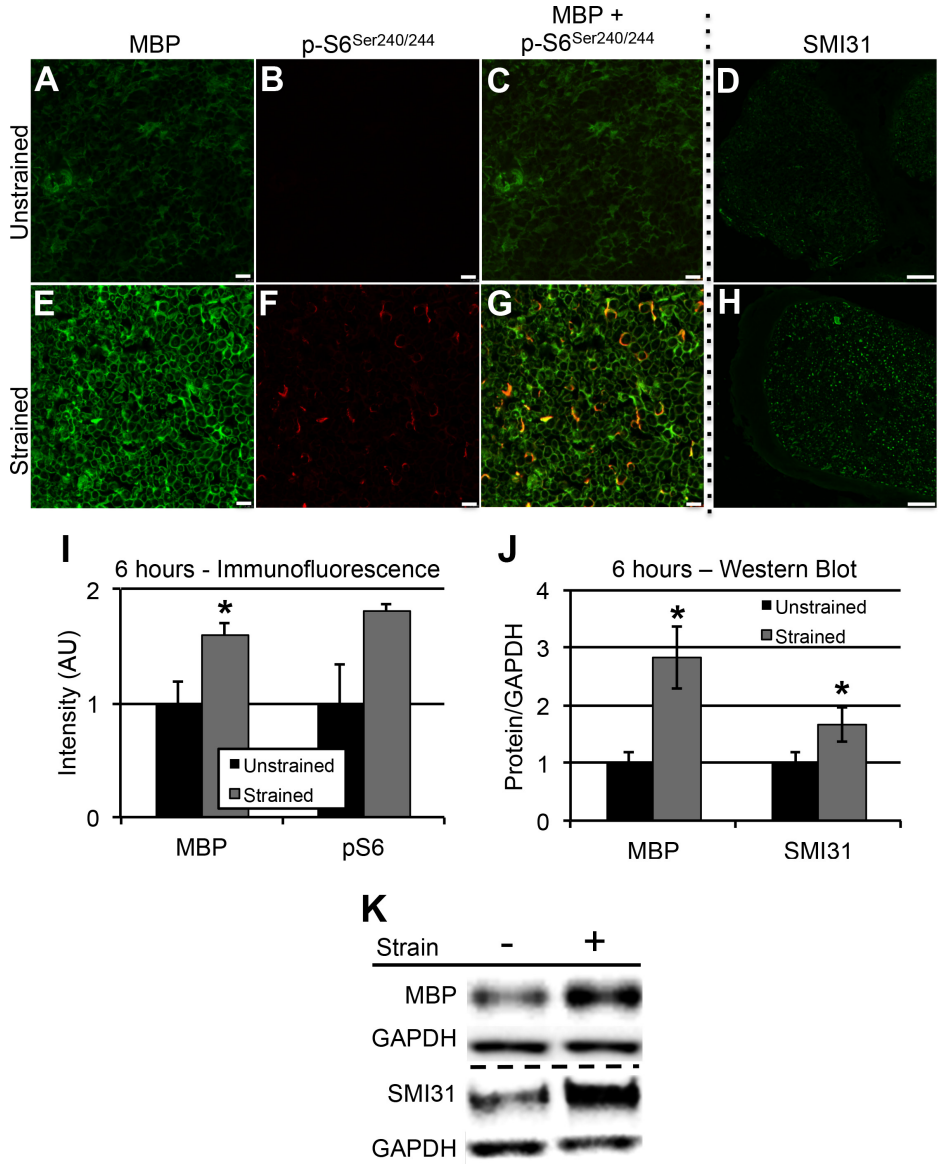

Fig. 3. Immunohistochemistry and Schwann cell signaling. Immunofluorescence of whole nerve cross sections revealed increases in MBP *(A* vs. *E)*, pS6 *(B* vs. *F)*, and SMI31 *(D* vs. *H)* with strain. Double-labeling of MBP and pS6 *(C* and *G)*, revealed that pS6 expression was primarily localized to myelin following nerve strain. Western blots confirmed strain-dependent increases in both MBP and SMI31 *(I–K)*, suggesting a role for Schwann cells in the response of nerves to strain. Scale bar = 10 μm for MBP and pS6 and 100 μm for SMI31.

effect ($P = 1.18\times10^{-6}$) and trend towards an interaction effect ($P = 0.074$) were observed, suggesting that mTOR activation may be disproportionately suppressed in strained nerves. Consistent with these data, S6 activation was also suppressed following rapamycin treatment in both the contralateral, unstrained limb (82% reduction; Fig. 4, *C* and *D*) and the strained nerve (85% reduction; Fig. 4, *C* and *D*). Two-way ANOVA also revealed a significant effect of rapamycin on S6 activation ($P = 8.89\times10^{-12}$). In this case there was no strain effect ($P = 0.15$), but a trend toward an interaction effect ($P = 0.0841$). Post hoc comparison of individual groups revealed a significant influence of strain in the absence of rapamycin, which disappears following rapamycin administration (no rapamycin, $P = 0.014$; rapamycin, $P = 0.632$). Rapamycin also resulted in decreased total mTOR and S6 (Fig. 4, *F* and *G*), suggesting that the resultant decrease in signaling reflected both reduced phosphorylation and reduced phosphorylable targets.

Rapamycin treatment revealed differential translational regulation of the probed cytoskeletal proteins. β-Actin expression remained elevated following strain application ($P = 0.027$; Fig. 4, *E* and *F*). However, NF-H ($P = 0.90$; Fig. 4, *E* and *F*) and Tuj1 ($P = 0.613$; Fig. 4, *E* and *F*) remained equal to those of the unstrained nerve. Total tubulin saw a significant decrease relative to the unstrained nerve (61% reduction; $P = 0.002$). In the presence of rapamycin, there was a suppression of the effect of strain on both MBP ($P = 0.183$; Fig. 4, *F* and *G*) and SMI31 ($P = 0.582$; Fig. 4, *F* and *G*), consistent with interplay between myelination and neurofilament phosphorylation.

Puromycin Identification of Strain-Induced Signaling in DRG Cultures

To test for increases in whole protein synthesis within in vitro neurons, embryonic DRGs were dissected and plated onto a flexible PDMS substrate. Immunolabeling after application of 20% strain for 1 h in the presence of puromycin allowed quantification of puromycin incorporated into newly synthesized proteins (Fig. 5). This measurement can be used as a surrogate for total protein synthesis during the experimental time course. Analysis of the puromycin ex-

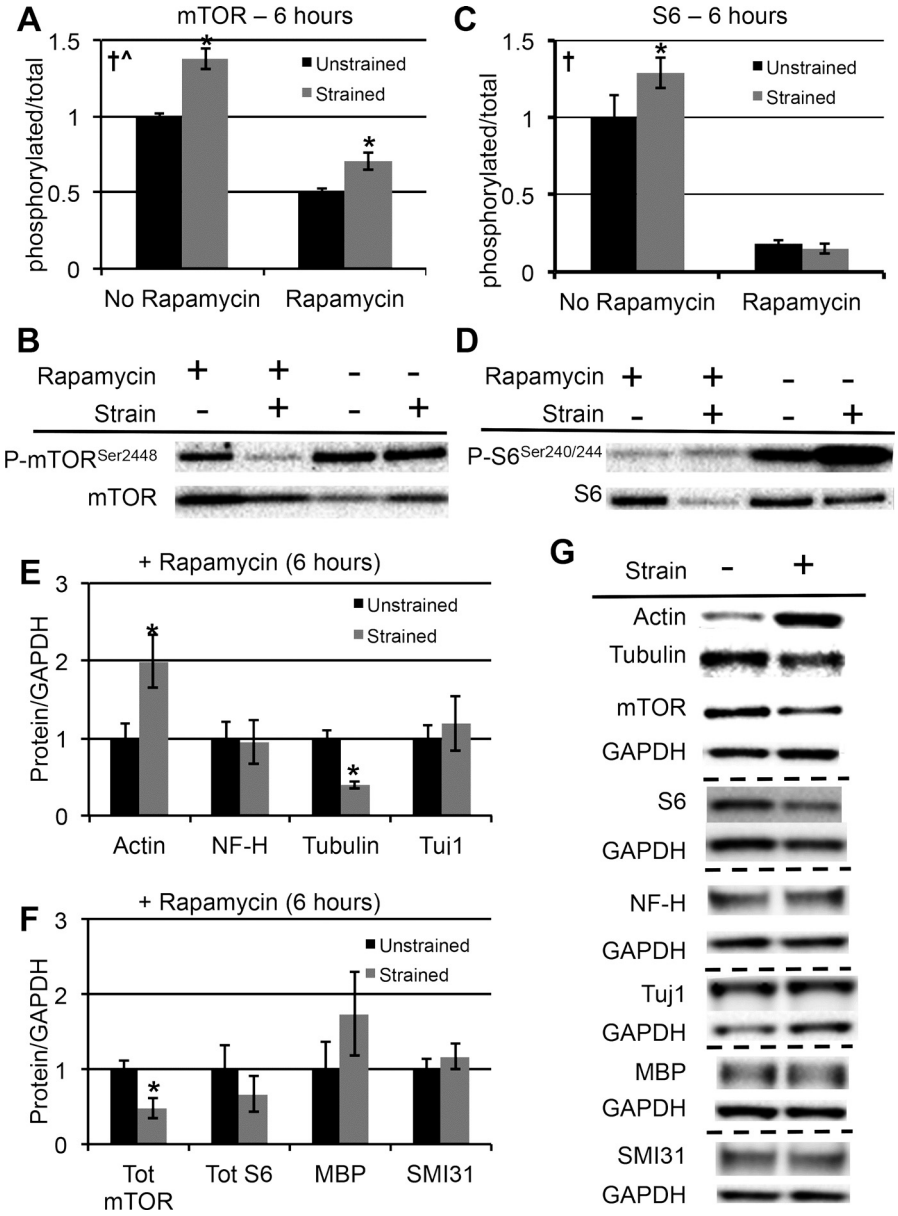

Fig. 4. Effect of rapamycin on strain-induced signaling and protein expression. Application of mTOR led to a reduction in phosphorylated levels of both mTOR (*A* and *B*) and S6 (*C* and *D*) (graphs normalized to unstrained, no-rapamycin group). The effect of strain remains following rapamycin administration but was muted at the level of S6. Administration of rapamycin before strain differentially regulated protein levels (*E* and *F*) (protein data normalized to unstrained, rapamycin treated): β-actin remained elevated and both tubulin and total mTOR were reduced beyond baseline. Total S6 levels were not significantly different from baseline. Strain effect on MBP and SMI31 reported previously was eliminated in presence of rapamycin. *G*: sample Western blots are shown for each protein of interest. $*P < 0.05$, paired *t*-test; 2-way ANOVA, effect of strain: $\wedge P < 0.05$, effect of rapamycin: $\dagger P < 0.05$; means ± SE.

pression in DRG axons following strain revealed an increase in mean pixel intensity in the axon, consistent with increased protein synthesis ($P = 0.042$; paired *t*-test, $N = 14$ cells from 3 different devices were sampled per group).

DISCUSSION

In this study, we implemented a new experimental model to examine translational pathways in response to nerve strain, in the absence of nerve injury. Our results suggest that strain induces alterations in Schwann cells and neuronal structure and composition, including mTOR-dependent increases in myelin basic protein levels and neurofilament phosphorylation.

Strain-Induced Signaling and Local Protein Synthesis

Although not a prototypical load-bearing tissue, nerves experience, accommodate, and respond to tensile deformations (Boyd et al. 2005; Kwan et al. 1992). In single neurons, moderate strains induce beneficial outcomes (Bray 1984; Lamoureux et al. 1998; Pfister et al. 2004), with one study reporting a dramatic nearly eightfold increase in axonal elongation rates (Pfister et al. 2004). In vivo, such loading is well described during normal joint movement, limb lengthening surgery (Boyd et al. 2005; Ikeda et al. 2000), and, more recently, strategies for end-to-end nerve repair (Hentz et al. 1993) and strain-based regenerative strategies (Abe et al. 2004; Chuang et al. 2013).

In vivo, axons themselves may, at least partially, be protected from nerve strain by their unique undulating packing architecture within the nerves as well as properties of the extracellular matrix (Kwan et al. 1992; Love et al. 2013; Phillips et al. 2004). However, when axons themselves are strained, in vivo or in vitro, details on how they respond to deformation are poorly understood. An important observation was that axons do not display reduced caliber with strain, indicating volumetric expansion as well as structural stability (Loverde et al. 2011). Additionally, limb-lengthening models

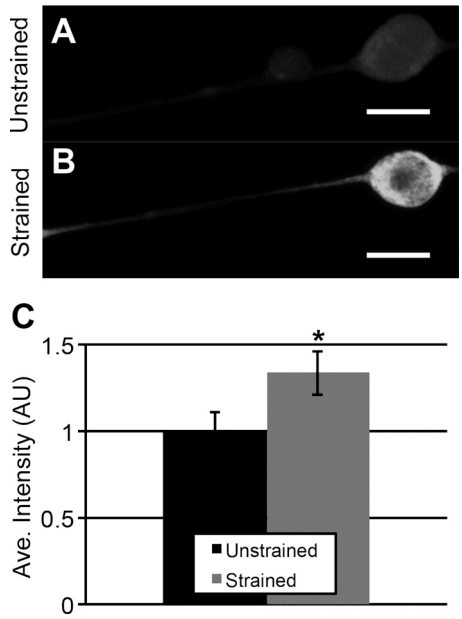

Fig. 5. In vitro puromycin incorporation increases in response to strain. In vitro incorporation of puromycin was identified by immunolabeling of both unstrained (*A*) and strained (*B*) samples. *C*: a significant increase in axonal fluorescent intensity was observed following a 1-h application of strain (*$P < 0.05$, paired *t*-test, $N = 14$ cells from 3 different devices per group); means ± SE; graph normalized to unstrained levels.

have revealed that strain induces elongation of internodes without a reduction in nerve fiber area or g-ratio, again suggesting volumetric expansion and in the cases of both neurons and Schwann cells (Abe et al. 2004; Abe et al. 2002). Multiple sources of cellular material may contribute to this expansion. In the short term, preexisting pools of cellular material may be rapidly recruited from neuronal or Schwann cell bodies, in a manner analogous to the anterograde cytoskeletal flow posited during axonal outgrowth (Dai and Sheetz 1995; Loverde et al. 2011). However, to accommodate long-term volume expansion additional material must be newly synthesized, either in the cell body or, as we hypothesize, locally within the axon.

mTOR signaling has not been investigated in the context of neuronal strain, but the mTOR/S6 pathway is a strong candidate for modulating strain-induced local protein synthesis, based on such a role in regulating skeletal muscle hypertrophy (Klossner et al. 2009). In neurons, mTOR pathways are known to be vitally important in axonal elongation (Abe et al. 2010; Lu et al. 2012; Park et al. 2010; Verma et al. 2005) and axonal branching (Grider et al. 2009), as well as nerve growth during development or regeneration (Ning et al. 2010; Park et al. 2010; Sherman et al. 2012; Verma et al. 2005); local protein synthesis is central to all of these processes (Zheng et al. 2001). In our study, we imparted strain without appreciably impairing neurovascular function (Fig. 1). We observed that strain induced a rapamycin-sensitive [i.e., mTOR complex 1 (mTORC1)-associated], rapid, and persistent increase in mTOR activation as well as downstream activation of S6 (Fig. 2, *A* and *B*). Given that strain-associated mTOR activation is often linked to FAK signaling, it was somewhat surprising that FAK activation did not increase, at both short and later time points; however, Akt signaling upstream of mTOR may be influenced by integrin- and laminin-associated signaling pathways such as integrin-linked-kinase pathways (Colognato et al. 2005), which represent alternate possibilities for upstream activation.

While any number of proteins may be regulated through mTOR-S6 pathways, we focused primarily on structural proteins, whose synthesis is essential to volume expansion (Fine and Bray 1971; Friede and Samorajski 1970; Hoffman and Lasek 1980). This effort does not exclude mTOR-mediated regulation of additional targets associated with growth, including mitochondrial metabolism or lipid synthesis (reviewed in Norrmén and Suter 2013). As also observed following nerve injury, β-actin levels increased following nerve strain; however, NF-H and total tubulin remained relatively unchanged with strain, suggesting a response different from that occurring during the regeneration of axonal sprouts, where neurofilament levels decrease (Bignami et al. 1986; Moss and Lewkowicz 1983; Pestronk et al. 1990).

Observed immunolocalization of activated S6 following strain suggested that substantial mTOR/S6 associated signaling occurs in myelinating Schwann cells (Fig. 3). A number of studies in the central nervous system positively identified a role for mTOR signaling in oligodendrocyte differentiation (Tyler et al. 2009) and myelination (Narayanan et al. 2009; Wahl et al. 2014), though MBP protein levels were not affected by rapamycin treatment. Conversely, our observed rapamycin-dependent increase in MBP protein levels after strain supports a role for mTOR signaling in Schwann cell growth, as demonstrated by reduced myelination, reduced g-ratio, and reduced axonal caliber following genetic reduction of mTOR (Sherman et al. 2012). Because it is not possible to completely decouple Schwann cell and neuronal response to strain in whole nerves, to test for neuron-specific influences of strain free from confounding signals from Schwann cells, we utilized an in vitro neuronal deformation system. Based on outcomes from a puromycin incorporation assay, we observed an increase in axonal protein synthesis with strain, suggesting that neurons themselves are also experiencing an increase in protein synthesis. This result is consistent with observations that levels of neuron specific β3-tubulin trended toward an increase with strain ($P < 0.08$). Though this comparison did not achieve statistical significance due to high variability in this particular readout, a deeper examination of neuron-specific translational signaling would be warranted and interesting. Such an examination might also include assessments of time-dependent changes in translational activity in cell bodies (in vitro and in vivo), and also an analysis of whether translated transcripts are produced within neurons themselves, or transcytose from neighboring Schwann cells (Court et al. 2008).

Our results provide additional evidence of the intertwined relationship between myelination and neurofilament phosphorylation. The intriguing phenomenon that Schwann cell myelination influences neurofilament phosphorylation was initially demonstrated in the Trembler mouse and in normal axons (de Waegh et al. 1992; Hsieh et al. 1994), which revealed reductions in P-NF-H in regions of decreased myelination. Consistent with these observations, we observed parallel increases in NF-H phosphorylation and MBP, with no change in overall NF-H levels, with strain. Though at a 6-h time point we cannot reliably assess the influence of these increases on myelination, their rapamycin dependence provides a mechanistic basis for the remarkable ability of nerves to accommodate moderate levels of strain, both with respect to maintaining normal ge-

ometry (Abe et al. 2004) and modifying their expression of myelin-associated proteins (Hara et al. 2003).

While rapamycin suppressed the effect of strain on MBP, tubulin, and NF-H phosphorylation, β-actin levels remained elevated, even following rapamycin administration. The maintained increase in levels of β-actin suggests that an alternative signaling pathway is responsible for either de novo synthesis of β-actin or local recruitment to the region of strain. One possibility is regulation of β-actin transport and translation via RNA binding proteins. A possible candidate for such regulation is zipcode binding protein 1 (ZBP1), a β-actin binding protein whose activity appears to be controlled by calcium-mediated Src pathways (Hüttelmaier et al. 2005; Yao et al. 2006). While further manipulation of non-mTOR pathways is necessary to conclude a formal role, our results leave open the compelling possibility of competing or synergistic transport-associated pathways. Indeed, a recent study on stretched DRG neurons revealed a slight increase in actin mobility following moderate strain (Bober et al. 2015).

Finally, we cannot exclude the possibility that both the cell body and flanking unstretched regions may provide material for axonal growth and response to strain; however at our 6-h time point, this contribution is likely to be minimal. Transport of cytoskeletal cargoes is well characterized as slow component transport, with bulk rates of β-actin, tubulin, and neurofilaments transport rarely exceeding 1 mm/day (Black and Lasek 1979; Hoffman and Lasek 1975). At these rates, 6 h is likely an insufficient amount of time for newly transported proteins to appreciably contribute to measured increases, which were on the order of 50%. It is a limitation of our work that we did not formally assess this possibility by examining waves of transport from the cell body over time, and this remains a possible set of experiments for future study.

Conclusions

It is well established that the application of excessive strain and tension on nerves has a major deleterious effect, which at the greatest extremes fully and irreversibly eliminates a nerve's conductive capacity while under load (Kwan et al. 1992; Wall et al. 1992). In our study, we successfully applied a moderate static strain to nerves in vivo, without incurring functional deficits. Application of strain led to increased mTOR signaling, levels of myelin-associated proteins, and neurofilament phosphorylation, providing another example of the interdependent relationship between myelinating Schwann cells and neuronal structure. Our in vitro data also suggest that neurons increase protein synthesis during the application of strain. Cumulatively, our work provides a putative mechanism for the nerve's ability to respond and adapt to strain. This has implications both for strain-based strategies for nerve repair as well as for the adaptation of untransected nerves, such as during development or nerve entrapment.

ACKNOWLEDGMENTS

We gratefully acknowledge helpful discussions with members of the Neuromuscular Bioengineering and Muscle Physiology Laboratories.

GRANTS

The authors received funding from NSF (CMMI1130997 and CBET1042522 to S. B. Shah), Department of Veterans Affairs (I01RX001471-01 to S. B. Shah), NIH (1R01AR059179 to R. M. Lovering), the UCSD Academic Senate (S. B. Shah), and the National Skeletal Muscle Research Center at UCSD (S. B. Shah).

DISCLOSURES

No conflicts of interest, financial or otherwise, are declared by the authors.

AUTHOR CONTRIBUTIONS

J.M.L. and S.B.S. conceived and designed research; J.M.L., B.G.B., E.O., A.T.W., and S.N.B. performed experiments; J.M.L., B.G.B., E.O., A.T.W., S.N.B., S.S., and S.B.S. analyzed data; J.M.L., B.G.B., E.O., A.T.W., S.N.B., R.M.L., S.S., and S.B.S. interpreted results of experiments; J.M.L. and S.B.S. prepared figures; J.M.L. and S.B.S. drafted manuscript; J.M.L., R.M.L., and S.B.S. edited and revised manuscript; J.M.L., B.G.B., E.O., A.T.W., S.N.B., R.M.L., S.S., and S.B.S. approved final version of manuscript.

REFERENCES

Abe I, Ochiai N, Ichimura H, Tsujino A, Sun J, Hara Y. Internodes can nearly double in length with gradual elongation of the adult rat sciatic nerve. *J Orthop Res* 22: 571–577, 2004. doi:10.1016/j.orthres.2003.08.019.

Abe I, Tsujino A, Hara Y, Ichimura H, Ochiai N. Paranodal demyelination by gradual nerve stretch can be repaired by elongation of internodes. *Acta Neuropathol* 104: 505–512, 2002.

Abe N, Borson SH, Gambello MJ, Wang F, Cavalli V. Mammalian target of rapamycin (mTOR) activation increases axonal growth capacity of injured peripheral nerves. *J Biol Chem* 285: 28034–28043, 2010. doi:10.1074/jbc.M110.125336.

Arnaoutoglou CM, Sakellariou A, Vekris M, Mitsionis GI, Korompilias A, Ioakim E, Harhantis A, Beris A. Maximum intraoperative elongation of the rat sciatic nerve with tissue expander: functional, neurophysiological, and histological assessment. *Microsurgery* 26: 253–261, 2006. doi:10.1002/micr.20236.

Bignami A, Chi NH, Dahl D. Neurofilament phosphorylation in peripheral nerve regeneration. *Brain Res* 375: 73–82, 1986. doi:10.1016/0006-8993(86)90960-1.

Black MM, Lasek RJ. Axonal transport of actin: slow component b is the principal source of actin for the axon. *Brain Res* 171: 401–413, 1979. doi:10.1016/0006-8993(79)91045-X.

Bober BG, Gutierrez E, Plaxe S, Groisman A, Shah SB. Combinatorial influences of paclitaxel and strain on axonal transport. *Exp Neurol* 271: 358–367, 2015. doi:10.1016/j.expneurol.2015.06.023.

Boyd BS, Puttlitz C, Gan J, Topp KS. Strain and excursion in the rat sciatic nerve during a modified straight leg raise are altered after traumatic nerve injury. *J Orthop Res* 23: 764–770, 2005. doi:10.1016/j.orthres.2004.11.008.

Bray D. Axonal growth in response to experimentally applied mechanical tension. *Dev Biol* 102: 379–389, 1984. doi:10.1016/0012-1606(84)90202-1.

Chuang TH, Wilson RE, Love JM, Fisher JP, Shah SB. A novel internal fixator device for peripheral nerve regeneration. *Tissue Eng Part C Methods* 19: 427–437, 2013. doi:10.1089/ten.tec.2012.0021.

Colognato H, ffrench-Constant C, Feltri ML. Human diseases reveal novel roles for neural laminins. *Trends Neurosci* 28: 480–486, 2005. doi:10.1016/j.tins.2005.07.004.

Court FA, Hendriks WT, MacGillavry HD, Alvarez J, van Minnen J. Schwann cell to axon transfer of ribosomes: toward a novel understanding of the role of glia in the nervous system. *J Neurosci* 28: 11024–11029, 2008. doi:10.1523/JNEUROSCI.2429-08.2008.

Dal J, Sheetz MP. Axon membrane flows from the growth cone to the cell body. *Cell* 83: 693–701, 1995. doi:10.1016/0092-8674(95)90182-5.

de Waegh SM, Lee VM, Brady ST. Local modulation of neurofilament phosphorylation, axonal caliber, and slow axonal transport by myelinating Schwann cells. *Cell* 68: 451–463, 1992. doi:10.1016/0092-8674(92)90183-D.

Dennerll TJ, Lamoureux P, Buxbaum RE, Heidemann SR. The cytomechanics of axonal elongation and retraction. *J Cell Biol* 109: 3073–3083, 1989. doi:10.1083/jcb.109.6.3073.

Donnelly CJ, Park M, Spillane M, Yoo S, Pacheco A, Gomes C, Vuppalanchi D, McDonald M, Kim HH, Merianda TT, Gallo G, Twiss JL. Axonally synthesized β-actin and GAP-43 proteins support distinct modes of axonal growth. *J Neurosci* 33: 3311–3322, 2013. doi:10.1523/JNEUROSCI.1722-12.2013.

Eng H, Lund K, Campenot RB. Synthesis of beta-tubulin, actin, and other proteins in axons of sympathetic neurons in compartmented cultures. *J Neurosci* 19: 1–9, 1999.

Eshleman JS, Carlson BL, Mladek AC, Kastner BD, Shide KL, Sarkaria JN. Inhibition of the mammalian target of rapamycin sensitizes U87 xenografts to fractionated radiation therapy. *Cancer Res* 62: 7291–7297, 2002.

Fine RE, Bray D. Actin in growing nerve cells. *Nat New Biol* 234: 115–118, 1971. doi:10.1038/newbio234115a0.

Friede RL, Samorajski T. Axon caliber related to neurofilaments and microtubules in sciatic nerve fibers of rats and mice. *Anat Rec* 167: 379–387, 1970. doi:10.1002/ar.1091670402.

Grider MH, Park D, Spencer DM, Shine HD. Lipid raft-targeted Akt promotes axonal branching and growth cone expansion via mTOR and Rac1, respectively. *J Neurosci Res* 87: 3033–3042, 2009. doi:10.1002/jnr.22140.

Hara Y, Shiga T, Abe I, Tsujino A, Ichimura H, Okado N, Ochiai N. P0 mRNA expression increases during gradual nerve elongation in adult rats. *Exp Neurol* 184: 428–435, 2003. doi:10.1016/S0014-4886(03)00259-0.

Hentz VR, Rosen JM, Xiao SJ, McGill KC, Abraham G. The nerve gap dilemma: a comparison of nerves repaired end to end under tension with nerve grafts in a primate model. *J Hand Surg Am* 18: 417–425, 1993. doi:10.1016/0363-5023(93)90084-G.

Hoffman PN, Lasek RJ. The slow component of axonal transport. Identification of major structural polypeptides of the axon and their generality among mammalian neurons. *J Cell Biol* 66: 351–366, 1975. doi:10.1083/jcb.66.2.351.

Hoffman PN, Lasek RJ. Axonal transport of the cytoskeleton in regenerating motor neurons: constancy and change. *Brain Res* 202: 317–333, 1980. doi:10.1016/0006-8993(80)90144-4.

Hsieh ST, Kidd GJ, Crawford TO, Xu Z, Lin WM, Trapp BD, Cleveland DW, Griffin JW. Regional modulation of neurofilament organization by myelination in normal axons. *J Neurosci* 14: 6392–6401, 1994.

Hüttelmaier S, Zenklusen D, Lederer M, Dictenberg J, Lorenz M, Meng X, Bassell GJ, Condeelis J, Singer RH. Spatial regulation of beta-actin translation by Src-dependent phosphorylation of ZBP1. *Nature* 438: 512–515, 2005. doi:10.1038/nature04115.

Ikeda K, Tomita K, Tanaka S. Experimental study of peripheral nerve injury during gradual limb elongation. *Hand Surg* 5: 41–47, 2000. doi:10.1142/S0218810400000028.

Iwata A, Browne KD, Pfister BJ, Gruner JA, Smith DH. Long-term survival and outgrowth of mechanically engineered nervous tissue constructs implanted into spinal cord lesions. *Tissue Eng* 12: 101–110, 2006. doi:10.1089/ten.2006.12.101.

Klossner S, Durieux AC, Freyssenet D, Flueck M. Mechano-transduction to muscle protein synthesis is modulated by FAK. *Eur J Appl Physiol* 106: 389–398, 2009. doi:10.1007/s00421-009-1032-7.

Kwan MK, Wall EJ, Massie J, Garfin SR. Strain, stress and stretch of peripheral nerve. Rabbit experiments in vitro and in vivo. *Acta Orthop Scand* 63: 267–272, 1992. doi:10.3109/17453679209154780.

Lamoureux P, Buxbaum RE, Heidemann SR. Axonal outgrowth of cultured neurons is not limited by growth cone competition. *J Cell Sci* 111: 3245–3252, 1998.

Love JM, Chuang TH, Lieber RL, Shah SB. Nerve strain correlates with structural changes quantified by Fourier analysis. *Muscle Nerve* 48: 433–435, 2013. doi:10.1002/mus.23809.

Loverde JR, Ozoka VC, Aquino R, Lin L, Pfister BJ. Live imaging of axon stretch growth in embryonic and adult neurons. *J Neurotrauma* 28: 2389–2403, 2011. doi:10.1089/neu.2010.1598.

Lu P, Wang Y, Graham L, McHale K, Gao M, Wu D, Brock J, Blesch A, Rosenzweig ES, Havton LA, Zheng B, Conner JM, Marsala M, Tuszynski MH. Long-distance growth and connectivity of neural stem cells after severe spinal cord injury. *Cell* 150: 1264–1273, 2012. doi:10.1016/j.cell.2012.08.020.

Moss TH, Lewkowicz SJ. The axon reaction in motor and sensory neurones of mice studied by a monoclonal antibody marker of neurofilament protein. *J Neurol Sci* 60: 267–280, 1983. doi:10.1016/0022-510X(83)90068-0.

Narayanan SP, Flores AI, Wang F, Macklin WB. Akt signals through the mammalian target of rapamycin pathway to regulate CNS myelination. *J Neurosci* 29: 6860–6870, 2009. doi:10.1523/JNEUROSCI.0232-09.2009.

Ning K, Drepper C, Valori CF, Ahsan M, Wyles M, Higginbottom A, Herrmann T, Shaw P, Azzouz M, Sendtner M. PTEN depletion rescues axonal growth defect and improves survival in SMN-deficient motor neurons. *Hum Mol Genet* 19: 3159–3168, 2010. doi:10.1093/hmg/ddq226.

Norrmén C, Suter U. Akt/mTOR signalling in myelination. *Biochem Soc Trans* 41: 944–950, 2013. doi:10.1042/BST20130046.

Olink-Coux M, Hollenbeck PJ. Localization and active transport of mRNA in axons of sympathetic neurons in culture. *J Neurosci* 16: 1346–1358, 1996.

Park KK, Liu K, Hu Y, Kanter JL, He Z. PTEN/mTOR and axon regeneration. *Exp Neurol* 223: 45–50, 2010. doi:10.1016/j.expneurol.2009.12.032.

Pestronk A, Watson DF, Yuan CM. Neurofilament phosphorylation in peripheral nerve: changes with axonal length and growth state. *J Neurochem* 54: 977–982, 1990. doi:10.1111/j.1471-4159.1990.tb02346.x.

Pfister BJ, Iwata A, Meaney DF, Smith DH. Extreme stretch growth of integrated axons. *J Neurosci* 24: 7978–7983, 2004. doi:10.1523/JNEUROSCI.1974-04.2004.

Phillips JB, Smit X, De Zoysa N, Afoke A, Brown RA. Peripheral nerves in the rat exhibit localized heterogeneity of tensile properties during limb movement. *J Physiol* 557: 879–887, 2004. doi:10.1113/jphysiol.2004.061804.

Restaino SM, Abliz E, Wachrathit K, Krauthamer V, Shah SB. Biomechanical and functional variation in rat sciatic nerve following cuff electrode implantation. *J Neuroeng Rehabil* 11: 73, 2014. doi:10.1186/1743-0003-11-73.

Schenk S, McCurdy CE, Philp A, Chen MZ, Holliday MJ, Bandyopadhyay GK, Osborn O, Baar K, Olefsky JM. Sirt1 enhances skeletal muscle insulin sensitivity in mice during caloric restriction. *J Clin Invest* 121: 4281–4288, 2011. doi:10.1172/JCI58554.

Schmidt EK, Clavarino G, Ceppi M, Pierre P. SUnSET, a nonradioactive method to monitor protein synthesis. *Nat Methods* 6: 275–277, 2009. doi:10.1038/nmeth.1314.

Sherman DL, Krols M, Wu L-MN, Grove M, Nave K-A, Gangloff Y-G, Brophy PJ. Arrest of myelination and reduced axon growth when Schwann cells lack mTOR. *J Neurosci* 32: 1817–1825, 2012. doi:10.1523/JNEUROSCI.4814-11.2012.

Sotelo-Silveira JR, Calliari A, Kun A, Benech JC, Sanguinetti C, Chalar C, Sotelo JR. Neurofilament mRNAs are present and translated in the normal and severed sciatic nerve. *J Neurosci Res* 62: 65–74, 2000. doi:10.1002/1097-4547(20001001)62:1<65::AID-JNR7>3.0.CO;2-Z.

Tetzlaff W, Bisby MA, Kreutzberg GW. Changes in cytoskeletal proteins in the rat facial nucleus following axotomy. *J Neurosci* 8: 3181–3189, 1988.

Tyler WA, Gangoli N, Gokina P, Kim HA, Covey M, Levison SW, Wood TL. Activation of the mammalian target of rapamycin (mTOR) is essential for oligodendrocyte differentiation. *J Neurosci* 29: 6367–6378, 2009. doi:10.1523/JNEUROSCI.0234-09.2009.

Verma P, Chierzi S, Codd AM, Campbell DS, Meyer RL, Holt CE, Fawcett JW. Axonal protein synthesis and degradation are necessary for efficient growth cone regeneration. *J Neurosci* 25: 331–342, 2005. doi:10.1523/JNEUROSCI.3073-04.2005.

Wahl SE, McLane LE, Bercury KK, Macklin WB, Wood TL. Mammalian target of rapamycin promotes oligodendrocyte differentiation, initiation and extent of CNS myelination. *J Neurosci* 34: 4453–4465, 2014. doi:10.1523/JNEUROSCI.4311-13.2014.

Wall EJ, Massie JB, Kwan MK, Rydevik BL, Myers RR, Garfin SR. Experimental stretch neuropathy. Changes in nerve conduction under tension. *J Bone Joint Surg Br* 74: 126–129, 1992.

Weiss P. Nerve patterns: the mechanics of nerve growth. *Growth* 5: 163–203, 1941.

Westerga J, Gramsbergen A. Changes in the electromyogram of two major hindlimb muscles during locomotor development in the rat. *Exp Brain Res* 92: 479–488, 1993. doi:10.1007/BF00229036.

White AT, McCurdy CE, Philp A, Hamilton DL, Johnson CD, Schenk S. Skeletal muscle-specific overexpression of SIRT1 does not enhance whole-body energy expenditure or insulin sensitivity in young mice. *Diabetologia* 56: 1629–1637, 2013. doi:10.1007/s00125-013-2912-2.

Yao J, Sasaki Y, Wen Z, Bassell GJ, Zheng JQ. An essential role for beta-actin mRNA localization and translation in Ca2+-dependent growth cone guidance. *Nat Neurosci* 9: 1265–1273, 2006. doi:10.1038/nn1773.

Zheng JQ, Kelly TK, Chang B, Ryazantsev S, Rajasekaran AK, Martin KC, Twiss JL. A functional role for intra-axonal protein synthesis during axonal regeneration from adult sensory neurons. *J Neurosci* 21: 9291–9303, 2001.